Colloid Polym Sci (2012) 290:1471–1480
DOI 10.1007/s00396-012-2673-3

ORIGINAL CONTRIBUTION

Chitosan nanostructures deposited from solutions in carbonic acid on a model substrate as resolved by AFM

Marina A. Khokhlova · Marat O. Gallyamov · Alexei R. Khokhlov

Received: 17 January 2012 / Revised: 11 April 2012 / Accepted: 25 April 2012 / Published online: 10 May 2012

Abstract Chitosan macromolecules can be dissolved in water saturated with CO_2 under high pressure, i.e. in carbonic acid. This unique biocompatible solvent with acidity regulated by the variation of applied CO_2 pressure is rather promising for biomedical applications. In this work the main features of deposition of chitosan structures on the model substrate from solutions in this media were examined. After deposition on the mica surface, the obtained structures have been successfully visualised by atomic force microscopy (AFM). It has been found out that they adsorb as rather peculiar elongated objects with an average length of about 70 nm. Such conformations are believed to appear due to amphiphilic nature of chitosan semi-flexible chains in agreement with recent theoretical findings. The well-defined geometry of the elongated monodispersed structures allows them to demonstrate some elements of liquid crystalline-like ordering.

Keywords Atomic force microscopy (AFM) · Carbonic acid · Chitosan · Coatings · Conformational analysis · Ordering

Introduction

Chitin is a very abundant natural polymer, and it can be converted easily into chitosan in large quantities. Chitosan is a biocompatible and non-toxic material possessing antimicrobial activity. Due to these properties, chitosan is very promising for biomedical applications, for example in formation of thin bio- and haemo-compatible coatings for artificial prostheses [1].

In our recent work, we focused on development of special chitosan coatings in order to improve stability and biocompatibility of artificial heart valves [2]. A long time ago, it was suggested that chitosan coatings should prevent their calcification [3]. Routine laboratory tests indeed typically demonstrate reduction of calcification due to influence of protective chitosan coatings on the bioprosthesis material [2–4]. The heart valve bioprostheses are usually produced from pericardial xenotissue stabilized by glutaraldehyde, which serves as a cross-linking agent imparting better mechanical properties and suppressing immune response. But such treatment leads to the occasional formation of free (i.e. unbound) aldehyde groups on the surface of biotissue. The residual free aldehyde groups are known to promote calcification [3, 4]. Polycationic chitosan coating should block such residual groups [3]. Additionally this coating is expected to impart antimicrobial activity to the pericardium surface as well as to prolong the durability of the artificial valves because of improved mechanical properties. Recently some other biocompatible cross-linking agents without any cytotoxicity have been proposed, such as genipin [5]. But when genipin is applied to cross-link the pericardium, no significant decrease of calcification in model experiments is detected as compared with cross-linking using glutaraldehyde [6]. Therefore, additional protection with chitosan coatings may be beneficial for the bioprostheses xenotissue stabilized by genipin and other cross-linking agents as well.

It would be very challenging to deposit protective polymer coatings from solutions in supercritical (sc) CO_2 for possible biomedical applications. Indeed, sc CO_2 is a hypoallergenic

M. A. Khokhlova (✉) · M. O. Gallyamov (✉) · A. R. Khokhlov
Faculty of Physics, Lomonosov Moscow State University,
Leninskie gory 1-2, GSP-1,
Moscow 119991, Russian Federation
e-mail: khokhlova@nano.msu.ru
e-mail: glm@spm.phys.msu.ru

M. A. Khokhlova · M. O. Gallyamov · A. R. Khokhlov
Nesmeyanov Institute of Organoelement Compounds RAS,
Vavilova 28, GSP-1,
Moscow 119991, Russian Federation

fluid, it produces no toxic or irritating residues in the modified tissue and after deposition of the coating it completely leaves the product [7]. Unfortunately, previously, we have found out that typical solubilities of chitosan or its derivatives in pure sc CO_2 are unacceptably low for real applications [8–10]. Therefore, in the present paper, we explore a completely different approach, namely, to deposit chitosan coatings from solutions in water saturated with CO_2 under high pressure (HP). Indeed, previously Sakai et al. [11] have already demonstrated that it is possible to dissolve chitosan with different degrees of acetylation (DAs) in water media for industrial applications if water is saturated with carbon dioxide and thus converted into carbonic acid. They achieved a perfect solubility for some chitosan gels and somewhat lower solubility for chitosan in powdery form. Taking into account these results, we expected better solubility of the polymer in carbonic acid as compared to sc CO_2. Carbonic acid is not a sc fluid; it is a "usual" liquid. Therefore, it does not possess the benefits of supercritical solvents. Nevertheless, carbonic acid beneficially combines two rather important properties: remaining biocompatibility and strong antimicrobial activity. Usually, a "biocompatible" solvent is also "compatible" with bacteria and viruses, thus special precautions should be taken to ensure bioclean conditions. For example, water is a hypoallergenic and biocompatible solvent either, but at normal conditions, it is a favourable environment for bacteria breeding (in particular, the surface of water). Carbonic acid with low pH values exists only at high pressures of CO_2 and possesses profound antimicrobial properties, i.e. it is not "compatible" with pathogens. Indeed, at high pressure, dissolved CO_2 molecules diffuse into bacteria, viruses and spores existing in water media and biologically inactivate them [7, 12–16]. The fact that water saturated with CO_2 under high pressure acquires most evident antimicrobial properties provides the fundamentally new method to control the balance between antimicrobial properties and biocompatibility of the solvent. This balance can be tuned in the absence of any chemical agents at all, only by means of purely physical factors (variable pressure). Thereby with this promising method, we totally escape from any possible immune, pyrogenic or other negative reactions of an organism related to the presence of some residual traces of chemical agents in the modified medical article. After dissolution of chitosan in this beneficial media with following deposition as a coating on a substrate, the pressure is to be reduced and as a result the carbonic acid is converted again into absolutely biocompatible and harmless for any organism mixture of H_2O and CO_2. Therefore, biocompatible properties are restored after decompression, and this fact is very encouraging for biomedical usage of carbonic acid. The decrease of the pressure not only converts the system back into the totally safe state, but also at these conditions chitosan loses its solubility, that provides the stability of the deposited coatings. Thus, no possible harmful residues should remain in the tissue after treatment. From the more general viewpoint, carbonic acid is an interesting example of a "physical solvent", whose acidity is to be regulated not by chemical composition, as usual, but by physically applied external CO_2 pressure. Therefore, usage of such solvent in chemical engineering processes—e.g. with cationic polymers—provides certain benefits that after treatment no neutralisation, washing out or dialysis is required for removal of anions. Indeed, after decrease of the applied pressure, the anions strongly tend to acquire protons and thus to turn spontaneously into H_2O and CO_2, which are to be removed easily.

In the present paper, we perform model deposition of chitosan structures from such solutions on atomically flat substrate (mica), suitable for the subsequent analysis with atomic force microscopy (AFM). This technique is rather popular in routine studies of conformational properties of single individual chains of many different polysaccharides [17–27], including chitosan [28]. Thus, the present study is aimed at investigation of the new approach of deposition of chitosan macromolecules from water saturated with CO_2, i.e. carbonic acid. Such experiments may contribute to better understanding of regularities determining the process of solubilisation and deposition of chitosan from solutions in carbonic acid.

Experimental

Materials

We used purified chitosan material from ZAO Sonat (Russia). The chitosan sample had 15 % degree of *N*-acetylation (DA) and the molecular weight M_n=90 kg/mol, M_w=160 kg/mol. Mica (muscovite; Plano GmbH, Germany) was used as a substrate for the deposition of polymer structures from prepared solutions in carbonic acid. In the experiments we used CO_2 of high purity (>99.997 %; Linde Gas Rus, Russia). We used water purified with a Millipore Milli-Q Synthesis system. The Milli-Q water was always freshly prepared just before usage.

Deposition of chitosan structures from solutions

The experimental HP setup was the same, as it was previously used for deposition of chitosan from solutions in sc CO_2 as described before [8–10]. Briefly, the HP setup consists of a pressure generator equipped with pressure sensors and a thermostatically controlled stainless steel HP reactor (inner volume 10 ml), which are united together by a set of capillaries. The setup can sustain the pressures of up to 80 MPa (as limited by the reactor).

The purity of the HP reactor was of an extreme importance for the success of the experiments on deposition of

ultra-small quantities of the chitosan material on an ultra-pure (freshly cleaved) mica substrate. The technique of purification of the reactor before each experiment as well as the purity control procedure was described earlier in details [8–10].

The deposition process was performed as follows. In the HP reactor, we put a freshly cleaved on both sides piece of mica with a surface area of about 1.5 cm^2 and some amount of chitosan (about 1 mg). The weight of the chitosan powder was measured by the Sartorius CP225D balance with the reproducibility of 0.02 mg. The half of the reactor (5 ml) was filled with Milli-Q water. The mica piece was completely immersed in the water phase located in the lower half of the reactor. The reactor was closed, tightened and purged with CO_2. Then it was filled with liquid CO_2 up to high pressure (30–35 MPa) at room temperature (23–25 °C) and left at this conditions for CO_2 dissolution and equilibration. The density of liquid CO_2 at such pressures and temperatures is equal to about 0.97–0.99 g/cm^3, as calculated using the "NIST Thermophysical Properties of Pure Fluids, ver. 3.1" program, i.e. it is still smaller as compared to water. So, liquid CO_2 phase is located in the upper half of the reactor. Therefore, the mica piece was exposed to carbonic acid in the lower half of the reactor, where the chitosan was gradually dissolving. The total exposure time was selected in the range of several days (2–14 days, but no significant difference in the results was observed for different exposure times within the range).

The exposure was finished also at room temperature by a rather slow decompression: the complete removal of non-dissolved CO_2 from the reactor took about 2–3 min. Next the substrate was retrieved from the disassembled reactor: the mica was taken out from the water phase, and the water excess was gently removed with filter paper, by touching the very edge of the mica piece. The thus obtained sample was dried at room humidity and then scanned with AFM.

The comparative deposition of chitosan from HCl solutions was performed in a manner modelling deposition from carbonic acid as close as possible. For the deposition we always prepared fresh solutions from dry powdery chitosan just before every experiment (one should better avoid any prolonged storage of aqueous solutions in the practice of AFM research). For that about 1 mg of chitosan, 1–30 μl of 30 % (T) HCl (Aldrich) and 5 ml of distilled H_2O were mixed in a clean flask and were equilibrated for 1–2 days. Then freshly cleaved mica was put in the solution and exposed for 1 day. After that mica was retrieved from the solution, again quickly dried with filter paper in the same manner as described above, dried at room humidity and scanned with AFM.

Deposition of chitosan structures from solutions

The AFM observations were carried out in a tapping mode in air at room conditions using a MultiMode microscope with a Nanoscope-IIIa controller (Digital Instruments, USA). AFM images were collected with an information density of 512×512 points at 1 Hz scanning frequency. We used silicon NCH-W cantilevers (NanoWorld AG, Switzerland) with a resonance frequency of about 320 kHz. According to the producer information, they ensure typical tip radius of curvature of less than 8 nm for these probes. Editing of the AFM images and image analysis were performed by means of NanoScope software (Digital Instruments) and FemtoScan Online (Advanced Technologies Center, Russia).

Results and discussion

Previously, we tested solubility in sc CO_2 of several different chitosan samples with different DAs (2–50 %) and after different pretreatments [8–10]. Some of the samples were completely insoluble in sc CO_2, others were sparingly soluble in this fluid, but we failed to achieve any significant solubility acceptable for real applications. The usage of liquid cosolvents (water, ethanol) has not yet allowed us to improve the solubility either. The best solubility in sc CO_2 was detected for the sample with DA 15 %. For comparison purposes, we selected this sample for the studies with carbonic acid reported in the present paper.

Therefore, we decided to switch from usage of sc CO_2 as a solvent to usage of water, saturated with CO_2 under high pressure, thus we followed the approach firstly suggested by Sakai et al. [11]. It is known that CO_2 at room temperature (25 °C) and at 30–40 MPa pressure demonstrates the solubility of about 3 mol% in water [29–33]. Further, the solubility of CO_2 in water increases with the increase of pressure [29–33]. Also, accordingly, the pH values decrease with the increase of pressure [34–37]. Therefore, one could expect the increase of the solubility of chitosan with the increase of pressure. Thus, Rinaudo et al. [38] demonstrated that there is a direct correlation between the amount of NH_2 groups required for protonation and the amount of protons available. Indeed, we found out that the solubility of chitosan in liquid water, saturated with CO_2 under high pressure, is much higher (up to, at least, 1 g/l) as compared to solubility of chitosan in dry (pure) or wet (with small amount of water) sc CO_2.

The macromolecular conformation as deposited from carbonic acid on a model mica substrate was rather peculiar (Fig. 1). Here we presented large-scale images to show general appearance of the deposited structures with film-like morphology (upper row of Fig. 1) as well as images of the same surface areas scanned again with reduced sizes in order to resolve fine structure of the elongated nanoparticles comprising the films (middle row of Fig. 1). Inserts in the lower row of Fig. 1 represent selected areas of these images

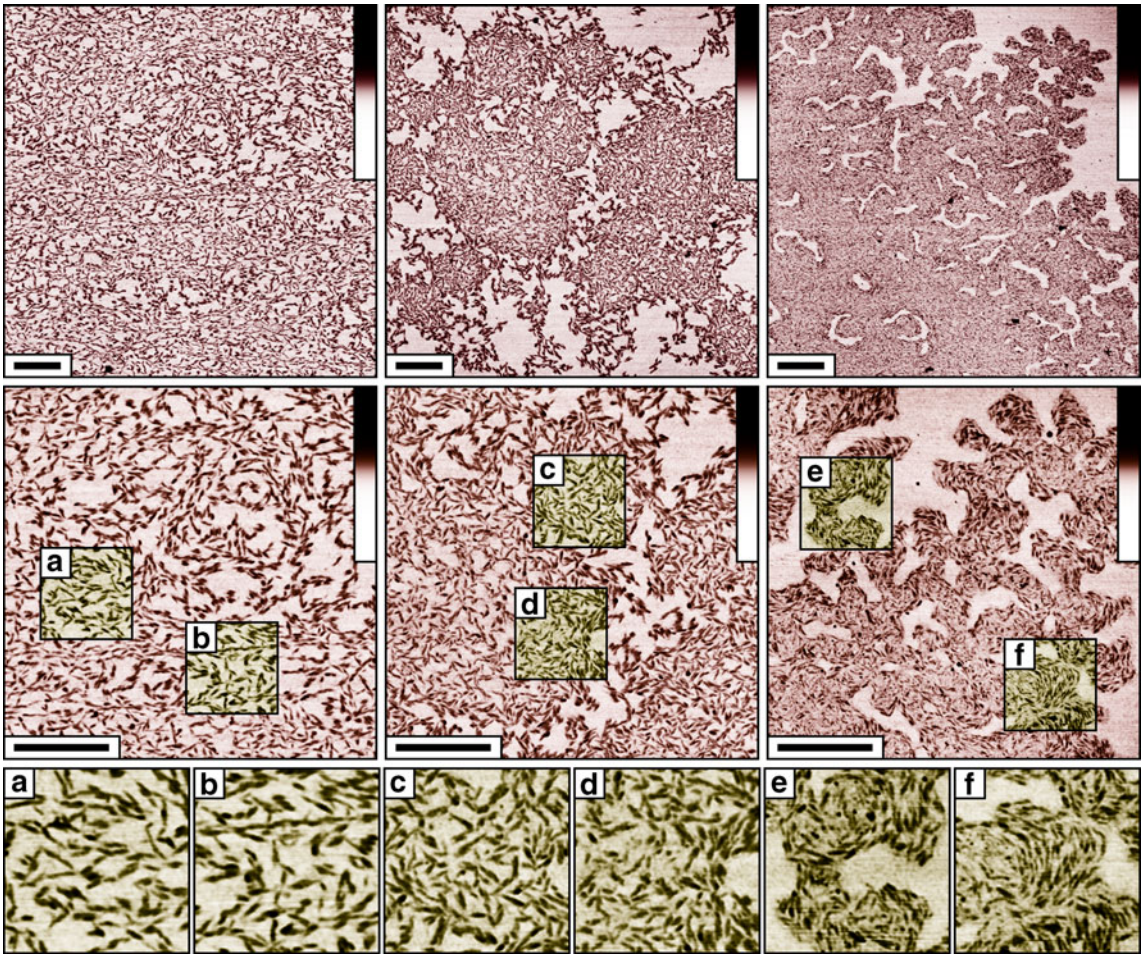

Fig. 1 Chitosan (15 % DA) nanostructures deposited on mica substrate from solutions in carbonic acid (water, saturated with CO_2 under high pressure, p=30 MPa, T=24 °C) as resolved by AFM. Chitosan concentration is equal to 0.2 g/l, CO_2 concentration is about 3 mol% [29–33], pH value is of about 2.8 [34–37]. Images in the *upper row* represent general morphology of the deposited films; scan sizes 4×4 μm^2. Images in the *middle row* represent the same surface areas re-scanned with smaller scan sizes (2×2 μm^2) in order to reveal individual particles comprising the films more clearly. Additionally, selected areas of these images are collected with an increased magnification in the *lower row*, as marked by (*a–f*) letters. *Scale bar* 500 nm, *height scale* 10 nm

with increased magnification. One can observe that the visualised here nano-sized objects resemble persistent rod-like structures.

The films we deposited were rather smooth and uniform, with nanometer-level thickness. They are composed by a single monolayer of the elongated persistent objects. The different images of Fig. 1 represent typical snapshots obtained for three different samples prepared at similar conditions, thus the similarity of the morphologies confirms reproducibility of the observations.

For the visualised persistent nano-sized structures, we measured systematically such parameters, as lengths, heights above the substrate level and widths at a half height, see Fig. 2. For the analysis we selected only isolated structures and we found out that their average length is equal to 70±20 nm (Fig. 2). The widths of adsorbed nano-objects at half height as measured with AFM are known to be systematically overestimated due to limited tip sharpness and true values are to be reconstructed using proper deconvolution algorithms [39]. We applied rather simple deconvolution procedure proposed by one of us a long time ago [40]. Briefly, the tip apex is modelled as a semisphere with the radius of 8 nm (see "Experimental" section) and the adsorbed object is represented as an oblate ellipsoid. The oblateness is due to certain deformation under the tip pressure and adhesion force to the substrate, but its degree is unknown a priori, i.e. before measurements and calculations. Then, from the geometry of the contact, it is possible to write an implicit equation for the real width of the object related to the values of its height, apparent (overestimated) width and tip radius. This implicit equation is to be solved numerically thus providing restored value of the real width. The precision of the calculation is very sensitive to the errors of the input data, that is rather typical situation for

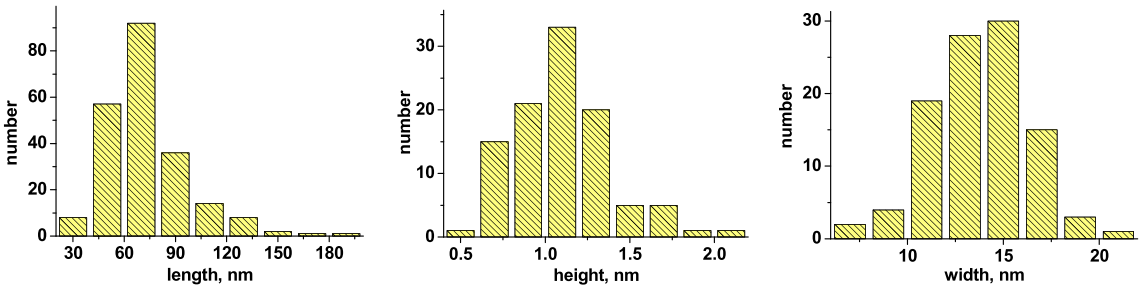

Fig. 2 Geometrical parameters as measured by AFM for the persistent rod-like structures of chitosan, deposited from solutions in carbonic acid (1 mg of chitosan, 5 ml of H_2O, saturated with CO_2 under pressure of 30 MPa and temperature 24 °C) including length, height and width (for the latter, the characteristics are presented as measured, i.e. overestimated due to limited tip sharpness)

solutions of inverse problems. Therefore, in order to supress statistically the uncertainty of the calculations, we accumulated sufficiently large statistics of $N=100$ measured pairs of the values of the height and apparent widths for different chitosan particles. Using this procedure we determined the reconstructed width values, which were found to be in the range of 9–14 nm. Taking into account the measured heights, lengths and reconstructed widths as well as their dispersion values, we estimated that the volume of a single persistent structure should be in the range of 300–1,000 nm^3. The rather large dispersion here is due to contribution of partial dispersions of all the three measured parameters including somewhat increased relative errors of widths after deconvolution procedure [40]. Comparing this range with the expected volume of one single chitosan chain (ca. 300 nm^3), we may conclude that the persistent structures may be composed by one to three macromolecules. Taking into account rather large uncertainty of the result of the deconvolution procedure, there are strong reasons to consider the visualised isolated persistent structures as monomolecular particles.

Carbonic acid as a solvent is rather unusual as compared with other typical aqueous solvents. Indeed, there is high pressure existing in the bulk, which might affect conformation of the dissolved macromolecules adsorbing on the substrate. In order to clarify the nature of the mechanism, which may cause such peculiar conformation of chitosan macromolecules, we performed a set of control experiments with deposition of the same chitosan macromolecules from HCl solutions at acidic pH values without any excessive pressure applied (laboratory conditions). It is well-known that chitosan is soluble in some aqueous acidic media, for example in formic, hydrochloric, acetic, lactic or propionic acids [41].

Firstly, with deposition from HCl solutions, we aimed to achieve nearly the same pH value of 2.8 [34–37] as in the experiments on deposition from chitosan solutions in water saturated with CO_2 under high pressure. But, unfortunately, reproducible AFM imaging was achieved only at pH values of about 2.0 and below. At the pH values of 1.8 for the chitosan material deposited from HCl aqueous solution, we typically detected two types of the deposited structures: (1) similar to the above-described elongated objects with comparable dimensions and (2) their aggregates of much larger sizes, see Fig. 3a. We were able to suppress aggregation during deposition rather efficiently only by decreasing pH down to the value of about 1.3. At such conditions the macromolecules are already deposited as well-isolated highly extended single chains, see Fig. 3b. The amount of the deposited material is significantly smaller at lower pH values (compare Fig. 3a, b). Indeed, only occasional separate chains are deposited at pH of 1.3. This strongly decreased ability of the macromolecules to adsorb at the fixed polymer concentration is apparently explained by the compensated charge of polyanionic mica surface at so low pH values. Still, the possibility to deposit extended single chains at such conditions is rather advantageous as far as it allows us to determine typical parameters of the extended macromolecular conformation—heights and lengths—as revealed by AFM for this particular chitosan sample. The measured average height of these extended macromolecules is equal to 0.55±0.17 nm above the mean substrate level (Fig. 3b). This value is in a good agreement with those reported previously for single chains of chitosan [28] and some other polysaccharides [42] from results of AFM measurements. Higher degree of extension as compared to

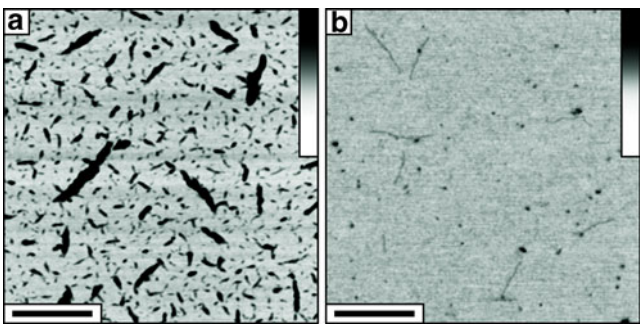

Fig. 3 Micrographs of chitosan structures on mica substrate deposited from solutions in hydrochloric acid at pH=1.8 (**a**), and at pH=1.3 (**b**); chitosan concentration=0.2 g/l; scan sizes 2×2 μm^2, *scale bar* 500 nm, *height scale* 10 nm

chitosan chains as typically deposited from acetate buffer [28] may be clearly related to the salt-free condition here, i.e. absence of any screening effects for the protonated amino groups. Indeed, the persistence length of these structures is much larger than the persistence length of single chitosan chains in solutions, which is reported to be in the range 9–13 nm [43]. This additional stiffness may be contributed by not only the electrostatic repulsion of the chitosan segments but also additionally by the interaction with the mica surface. The measured number average contour length of these extended chains is slightly above 200 nm value, which is in reasonable correlation with the molecular weight of the chitosan sample (M_n).

Regarding very peculiar morphology of chitosan macromolecules (Fig. 1) as deposited from solutions in carbonic acid, we may propose the following model of their assembly, comparing the relevant dimensions with those obtained for single chains as deposited from hydrochloric acid (Fig. 3b). The measured heights (1.1±0.3 nm) of the regular rod-like structures (Fig. 1) above the substrate level are two times larger as compared with the measured heights (0.55±0.17 nm) of the plainly adsorbed single isolated chitosan chains (Fig. 3b). The mean measured lengths (ca. 70 nm) of the particles (Figs. 1 and 2) are correspondingly three times smaller as compared with the mean measured lengths (ca. 200 nm) of the extended single chains (Fig. 3b). This is evidently indicative of intramolecular folding of the chitosan chains in the former case. We may propose the following model of their organisation, as depicted in Fig. 4, taking into account their elongated morphology and the results of reconstructions of volumes from AFM measurement (see above).

From comparison of Fig. 1 with Fig. 3a, it is clear that at similar depositing conditions, hydrochloric acid is much less effective in suppressing intermolecular aggregation as compared to carbonic acid. The observed higher efficiency of carbonic acid as compared to hydrochloric acid in breaking apart of intermolecular aggregates even at larger pH values may be explained by different factors. Firstly, the contribution may be due to higher intensity of fluctuations in this solvent. Indeed, due to very low apparent acidity constant of dissolved carbon dioxide, the water must be highly saturated with CO_2 molecules in order to achieve sufficient amount of anions and protons for pH=2.8 [44]. This low apparent acidity constant requires huge excess of CO_2 molecules as compared to anions. High amount of the dissolved CO_2 at high pressures ensures strong local fluctuations of the composition in the complex solution. As a result of the increased fluctuations intensity, the dispersing ability of the fluid is enhanced and this results in smaller degree of aggregation of chitosan macromolecules.

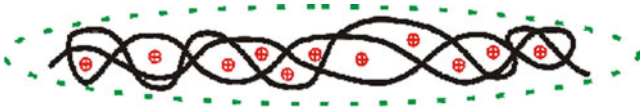

Fig. 4 Hypothetical folded elongated structure of a semiflexible chitosan chain in carbonic acid

Secondly, let us consider some other possible contributions towards the observed difference in the conformation of chitosan chains as deposited at similar conditions from solutions in carbonic (Fig. 1) and hydrochloric (Fig. 3a) acids. It should be related to rather complex conformational behaviour of polyelectrolyte chains, which is known to depend on many different parameters [45, 46] including the character of interaction between monomer units and their interaction with the solvent, on the fraction of charged units, on the valence and nature of counterions, on the dielectric properties of the solvent and even on the substrate influence as well [47]. AFM visualisation of adsorbed single chains is routinely explored nowadays to verify theoretical predictions on the rich conformational behaviour of polyelectrolyte macromolecules [48–51].

Let us estimate some relevant parameters. The dielectric constant of the rather diluted hydrochloric acid solutions as used in the present work is almost the same as for pure water, i.e. ε_{HCl} is equal to about 78 [52–54]. The corresponding Bjerrum lengths (l_B), may be calculated using the following equation:

$$l_B = \frac{e^2}{\varepsilon_S k_B T} \tag{1}$$

where e is the elementary electric charge, ε_S is the dielectric constant of the solvent, k_B is the Boltzmann constant and T is the temperature. Therefore, the Bjerrum length is of about 7.2 Å for the hydrochloric acid solutions.

Now, let us calculate the same parameter for carbonic acid solutions. Carbonic acid is a peculiar acid with dielectric properties variable by external CO_2 pressure. Indeed, it is an aqueous (polar) medium highly saturated with dissolved nonpolar CO_2 molecules. Yet, we failed to find direct experimental data on dielectric constant of carbonic acid in literature. Therefore we used Kirkwood equation [55] in order to calculate the dielectric constant of H_2O+CO_2 mixture, ε:

$$\frac{(\varepsilon-1)(2\varepsilon+1)}{9\varepsilon} = \rho\frac{P_1x_1 + P_2x_2}{M_1x_1 + M_2x_2} \tag{2}$$

where ρ is the density, P_i are the molar polarisations, x_i are the molar fractions and M_i are the molecular weights of the mixture components, i.e. of CO_2 and H_2O, respectively. When calculating ε of mixture, we neglect excess volume of mixing that is reasonable for such rather diluted solutions (x_{CO_2}=0.03 [29–33]). Calculation of molar polarisation for water is rather straightforward (2). In order to calculate the molar polarisation for liquid CO_2 (2) we used density value of ρ_{CO_2}=0.97 g/cm^3

(p=30 MPa, T=25 °C) as provided by the "NIST Thermophysical Properties of Pure Fluids" program and dielectric constant value of ε_{CO_2}=1.6 according to refs. [56, 57]. Following the Kirkwood approach [55], we obtained the value of $\varepsilon_{H_2O+CO_2}$=72 for the carbonic acid solution. This value correlates rather well with the data on typical static permittivity values of aqueous solutions with certain constituents (solutes) of rather different nature (including nonpolar molecules) at similar molar composition (x_i=0.03) [58, 59]. Taking into account the obtained value of $\varepsilon_{H_2O+CO_2}$, the corresponding Bjerrum length (1) for carbonic acid is equal to about 7.8 Å, i.e. it is only slightly larger as compared to the one for hydrochloric acid.

Knowing average monomer unit length for chitosan (b=5.2 Å) [8], we estimate that the characteristic relationship of $1.1\times l_B/b$ is equal to about 1.5 for hydrochloric acid and to about 1.6 for carbonic acid solutions. According to the phase diagram for a polyelectrolyte chain in a poor solvent developed in ref. [60] and taking into account the fraction of charged monomer units for the chitosan sample (f=0.85), we obtain that both values should correspond to the stretched chains region. But chitosan is a rather peculiar polyelectrolyte with strong tendency to form intensively intra- and inter-chain hydrogen bonding and thus one should hardly expect here exact coincidence with the borders between regions of the rather general phase diagram, which was calculated within assumption of Lennard-Jones attracting potentials for the interacting monomer units [60].

Thus, what we observed experimentally for the deposits from solutions in carbonic acids (Fig. 1) should be related apparently to the region of "sausage-like" or "cigar-like" [61] shapes of the same phase diagram [60]. This region corresponds to the increased Manning condensation of counterions reducing total net charge of polyelectrolyte chains. Indeed, the Manning condensation conditions [62]:

$$\xi = \frac{l_B f}{b} > 1 \qquad (3)$$

are met both for carbonic (ξ=1.3) and hydrochloric (ξ=1.2) acids. As a result of the charge compensation, the chitosan chains may adopt more compact conformation when, apart from repulsive electrostatic forces, there is distinct attraction between the monomer units due to contribution of mutual hydrogen bonding and dipole–dipole interaction of the coupled ion pairs. Further, the deposits from solutions in hydrochloric acid at similar conditions (Fig. 3a) also resemble such shapes, but additionally with highly increased tendency towards aggregation. This strongly increased aggregation may be explained by more effective ion pair formation when Cl^- ions serve as counterions as compared to HCO_3^-. Indeed, we believe that the affinity of protonated NH_3^+– groups towards Cl^- is much stronger then towards HCO_3^-. One can assume that from comparison of stability and chemical properties of well-known ammonium chloride and ammonium bicarbonate compounds. Thus, more effective coupling of the chitosan amino groups with the counterions in hydrochloric acid should be responsible for the increased contribution of dipole–dipole attraction between the condensates and therefore strongly amplified degree of their aggregation during deposition. Finally, the macromolecular tendency to adopt compacted/folded conformation because of reduced electrostatic repulsion due to counterion condensation effect is quite straightforward and natural to be expected.

The macromolecular packing into very similar folded particles was addressed recently for a rather general model of a macromolecule with just amphiphilic units in a selective solvent [63–65]. Depending on the macromolecular rigidity (L_k, intrinsic Kuhn segment lengths), different shapes were described: flexible chains formed linear strands of nearly spherical blobs, stiff chains organised into toroidal particles, whereas chains with intermediate rigidity twisted into "collagen-like" structures very much resembling the model of folding as depicted in Fig. 4 [63–65]. The typical L_k values for chitosan chains [66] correspond exactly to the intermediate range, thus formation of "collagen-like" structures should be expected according to the results of refs. [63–65]. In the packing model of such structures, the twisting chain folds over itself and its parts should wind around each other [63–65]. It is clear that such packing model coincides rather well with our observation of the rod-like particles (Fig. 1), taking into account their increased heights and decreased lengths as compared to "normal" extended chains (Fig. 3b). Similar rod-like globular structures were detected in water–alcohol solutions of Nafion macromolecules using methods of small-angle neutron and X-ray scattering [67]. The driving force for such packing at reduced electrostatic repulsion is the competition between macromolecular tendency to prevent all hydrophobic groups from contact with water and still to localise the amphiphilic units at

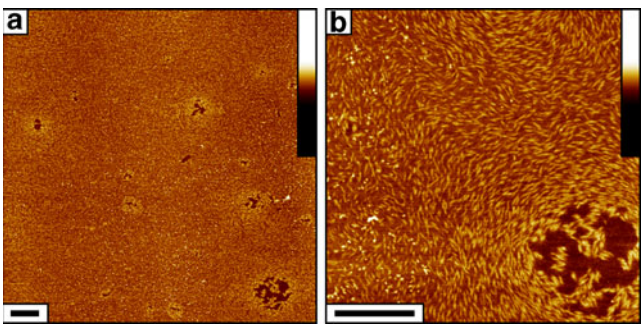

Fig. 5 Chitosan (15 % DA) nanostructures deposited on mica substrate from solutions in carbonic acid as resolved by AFM. Deposition conditions are similar to the described for Fig. 1. **a** General morphology of the deposited film; scan size 6×6 μm^2. **b** The same surface areas re-scanned with smaller scan size (2×2 μm^2) in order to reveal individual particles comprising the films more clearly. Some elements of liquid crystalline-like ordering in the film may be observed. *Scale bar* 500 nm, *height scale* 10 nm

the interface in contact with water, therefore formation of spherical globules may not provide sufficient surface places for all the amphiphilic units.

Thus, chitosan macromolecules in carbonic acid are folded and form well-defined nanoparticles of elongated morphology (Fig. 4). Their geometry is strongly asymmetric, i.e. the degree of extension is rather high. Strong regularity and high monodispersity of these well-defined very elongated particles quite naturally should provide possibility of their liquid crystalline-like ordering in condensed films [68]. Indeed, at rather large degrees of surface coverage for the deposited monolayer films, we clearly observed spontaneous liquid crystalline-like packing of the chitosan particles with pronounced local short-range ordering (see Fig. 5). The elongated structures form regular circularly oriented patterns around local defects in the film structure (Fig. 5), which resemble typical streamlines in the vicinity of circular defects in two-dimensional liquid crystalline films [69].

There is some distance between the deposited particles, as seen in Fig. 5, which may be indicative of electrostatic repulsion between them during adsorption. This is quite natural for the polyelectrolyte particles taking into account not complete local compensation of their charge. Such Coulomb contribution at certain conditions may promote ordering of the isotropic phase [70] as well as the ordering may be also induced by shear flow during evaporation at the solvent removal stage [71].

Our recent preliminary results (to be published elsewhere) indeed show that this tendency of the elongated chitosan particles to form ordered structures may be controlled and enhanced in order to produce liquid crystalline films of chitosan as cast from solutions in carbonic acid. Also, well-resolved spiral macroscopic organisation typical for *cholesteric* liquid crystals [72] was clearly observed in such the cast films. Therefore we may suppose chirality of the twisted chitosan rod-like particles, which have been visualised by AFM in the present paper (Fig. 1).

Conclusion

In the present study, we address the promising approach to deposit chitosan coatings from water saturated with CO_2 under high pressure. We found out that during deposition from solutions in the carbonic acid on a model substrate chitosan, amphiphilic macromolecules self-organise into elongated rod-like structures of apparently monomolecular composition. The main reason for this macromolecular folding into rod-like particles is related to the reduced electrostatic intrachain repulsion and amphiphilic nature of semiflexible chitosan chains in carbonic acid. The dissolving power of the carbonic acid may be apparently further increased by applying higher CO_2 pressures. It is interesting to emphasise that the well-defined morphology of the chitosan nanoparticles with high degree of asymmetry ensures local liquid crystalline-like ordering of 2D chitosan films as deposited from carbonic acid solutions. This ordering correlates with regular macroscopic organisation of much thicker 3D chitosan films as cast from this solvent.

Acknowledgments This work was supported by the Russian Academy of Sciences within the Basic Research Programme of the Division of Chemistry and Materials Sciences (Programme No OKh-3), and by Russian Foundation for Basic Research (Project No 10-03-00886a).

References

1. Pavinatto FJ, Caseli L, Oliveira ON (2010) Chitosan in nanostructured thin films. Biomacromolecules 11:1897–1908. doi:10.1021/bm1004838
2. Gamzazade AI, Bakuleva NP, Belavtseva EM, Gallyamov MO (2009) Electron microscopy of the coating morphology of pericardium tissue with chitosan ionogen derivatives. Bull Russ Acad Sci Phys 73:468–470. doi:10.3103/S1062873809040066
3. Chanda J (1994) Anticalcification treatment of pericardial prostheses. Biomaterials 15:465–469. doi:10.1016/0142-9612(94)90226-7
4. Nogueira GM, Rodas ACD, Weska RF, Aimoli CG, Higa OZ, Maizato M, Leiner AA, Pitombo RNM, Polakiewicz B, Beppu MM (2010) Bovine pericardium coated with biopolymeric films as an alternative to prevent calcification: in vitro calcification and cytotoxicity results. Mater Sci Eng C 30:575–582. doi:10.1016/j.msec.2010.02.011
5. Muzzarelli RAA (2009) Genipin-crosslinked chitosan hydrogels as biomedical and pharmaceutical aids. Carbohydr Polym 77:1–9. doi:10.1016/j.carbpol.2009.01.016
6. Chang Y, Tsai C, Liang H, Sung H (2002) In vivo evaluation of cellular and acellular/bovine pericardia fixed with a naturally occurring crosslinking agent (genipin). Biomaterials 23:2447–2457. doi:10.1016/S0142-9612(01)00379-9
7. Ellis JL (2010) Supercritical CO_2 sterilization of ultra-high molecular weight polyethylene. J Supercrit Fluids 52:235–240. doi:10.1016/j.supflu.2010.01.002
8. Gallyamov MO, Chaschin IS, Gamzazade AI, Khokhlov AR (2008) Chitosan molecules deposited from supercritical carbon dioxide on a substrate: visualization and conformational analysis. Macromol Chem Phys 209:2204–2212. doi:10.1002/macp.200800419
9. Khokhlova MA, Chaschin IS, Grigorev TE, Gallyamov MO (2010) Chitosan macromolecules on a substrate: deposition from solutions in sc CO_2 and reorganisation in vapours. Macromol Symp 296:531–540. doi:10.1002/masy.201051070
10. Chaschin IS, Grigorev TE, Gallyamov MO, Khokhlov AR (2012) Direct deposition of chitosan macromolecules on a substrate from solutions in supercritical carbon dioxide: solubility and conformational analysis. Eur Polym J. 48:906–918. doi:10.1016/j.eurpolymj.2012.03.003
11. Sakai Y, Hayano K, Yoshioka H, Yoshioka H (2001) A novel method of dissolving chitosan in water for industrial applications. Polym J 33:640–642. doi:10.1295/polymj.33.640
12. Bertoloni G, Bertucco A, De Cian V, Parton T (2006) A study on the inactivation of micro-organisms and enzymes by high pressure CO_2. Biotechnol Bioeng 95:155–160. doi:10.1002/bit.21006
13. Cinquemani C, Boyle C, Bach E, Schollmeyer E (2007) Inactivation of microbes using compressed carbon dioxide—an environmentally sound disinfection process for medical fabrics. J Supercrit Fluids 42:392–397. doi:10.1016/j.supflu.2006.11.001

14. Parton T, Bertucco A, Elvassore N, Grimolizzi L (2007) A continuous plant for food preservation by high pressure CO_2. J Food Eng 79:1410–1417. doi:10.1016/j.jfoodeng.2006.04.023
15. Parton T, Elvassore N, Bertucco A, Bertoloni G (2007) High pressure CO_2 inactivation of food: a multi-batch reactor system for inactivation kinetic determination. J Supercrit Fluids 40:490–496. doi:10.1016/j.supflu.2006.07.022
16. Qiu Q-Q, Leamy P, Brittingham J, Pomerleau J, Kabaria N, Connor J (2009) Inactivation of bacterial spores and viruses in biological material using supercritical carbon dioxide with sterilant. J Biomed Mater Res B Appl Biomater 91B:572–578. doi:10.1002/jbm.b.31431
17. Yokota S, Ueno T, Kitaoka T, Wariishi H (2007) Molecular imaging of single cellulose chains aligned on a highly oriented pyrolytic graphite surface. Carbohydr Res 342:2593–2598. doi:10.1016/j.carres.2007.08.018
18. Herasimenka Y, Cescutti P, Noguera CES, Ruggiero JR, Impallomeni G, Zanetti F, Campidelli S, Prato M, Rizzo R (2008) Macromolecular properties of cepacian in water and in dimethylsulfoxide. Carbohydr Res 343:81–89. doi:10.1016/j.carres.2007.10.003
19. Wang X, Xu X, Zhang L (2008) Thermally induced conformation transition of triple-helical lentinan in NaCl aqueous solution. J Phys Chem B 112:10343–10351. doi:10.1021/jp802174v
20. Wang J, Xu X, Zheng H, Li J, Deng JC, Xu Z, Chen J (2009) Structural characterization, chain conformation, and morphology of a β (1→3)-D-glucan isolated from the fruiting body of *Dictyophora indusiata*. J Agric Food Chem 57:5918–5924. doi:10.1021/jf9009872
21. Kobori T, Matsumoto A, Sugiyama S (2009) pH-dependent interaction between sodium caseinate and xanthan gum. Carbohydr Polym 75:719–723. doi:10.1016/j.carbpol.2008.10.008
22. Sletmoen M, Naess SN, Stokke BT (2009) Structure and stability of polynucleotide-(1,3)-beta-D-glucan complexes. Carbohydr Polym 76:389–399. doi:10.1016/j.carbpol.2008.10.035
23. Sletmoen M, Stokke BT (2009) Single-molecule pair studies of the interactions of the alpha-GalNAc (Tn-antigen) form of porcine submaxillary mucin with soybean agglutinin. Biopolymers 89:310–321. doi:10.1002/bip.21213
24. Funami T (2010) Atomic force microscopy imaging of food polysaccharides. Food Sci Technol Res 16:1–12. doi:10.3136/fstr.16.1
25. Zhang M (2010) Heating-induced conformational change of a novel β-(1→3)-D-glucan from *Pleurotus geestanus*. Biopolymers 93:121–131. doi:10.1002/bip.21303
26. Jones OG, Adamcik J, Handschin S, Bolisetty S, Mezzenga R (2010) Fibrillation of β-lactoglobulin at low ph in the presence of a complexing anionic polysaccharide. Langmuir 26:17449–17458. doi:10.1021/la1026619
27. Morris VJ, Gromer A, Kirby AR, Bongaerts RJM, Gunning AP (2011) Using AFM and force spectroscopy to determine pectin structure and (bio)functionality. Food Hydrocoll 25:230–237. doi:10.1016/j.foodhyd.2009.11.015
28. Kocun M, Grandbois M, Cuccia LA (2011) Single molecule atomic force microscopy and force spectroscopy of chitosan. Colloids Surf B Biointerfaces 82:470–476. doi:10.1016/j.colsurfb.2010.10.004
29. Wiebe R (1941) The binary system carbon dioxide-water under pressure. Chem Rev 29:475–481. doi:10.1021/cr60094a004
30. King MB, Mubarak A, Kim JD, Bott TR (1992) The mutual solubilities of water with supercritical and liquid carbon-dioxide. J Supercrit Fluids 5:296–302. doi:10.1016/0896-8446(92)90021-B
31. Teng H, Yamasaki A, Chun M-K, Lee H (1997) Solubility of liquid CO_2 in water at temperatures from 278 K to 293 K and pressures from 6.44 MPa to 29.49 MPa and densities of the corresponding aqueous solutions. J Chem Thermodynamics 29:1301–1310. doi:10.1006/jcht.1997.0249
32. Diamond LW, Akinfiev NN (2003) Solubility of CO_2 in water from −1.5 to 100 °C and from 0.1 to 100 MPa: evaluation of literature data and thermodynamic modelling. Fluid Phase Equilibria 208:265–290. doi:10.1016/S0378-3812(03)00041-4
33. Spycher N, Pruess K, Ennis-King J (2003) CO_2–H_2O mixtures in the geological sequestration of CO_2. I. Assessment and calculation of mutual solubilities from 12 to 100 °C and up to 600 bar. Geochim Cosmochim Acta 67:3015–3031. doi:10.1016/S0016-7037(03)00273-4
34. Meyssami B, Balaban MO, Teixeira AA (1992) Prediction of pH in model systems pressurized with carbon-dioxide. Biotechnol Prog 8:149–154. doi:10.1021/bp00014a009
35. Toews KL, Shroll RM, Wai CM (1995) pH-defining equilibrium between water and supercritical CO_2. Influence on SFE of organics and metal-chelates. Anal Chem 67:4040–4043. doi:10.1021/ac00118a002
36. Roosen C, Ansorge-Schumacher M, Mang T, Leitner W, Greiner L (2007) Gaining pH-control in water/carbon dioxide biphasic systems. Green Chem 9:455–458. doi:10.1039/b613345b
37. Schaef HT, McGrail BP, Owen AT (2010) Carbonate mineralization of volcanic province basalts. Int J Greenh Gas Control 4:249–261. doi:10.1016/j.ijggc.2009.10.009
38. Rinaudo M, Pavlov G, Desbrieres J (1999) Solubilization of chitosan in strong acid medium. Int J Polym Anal Charact 5:267–276. doi:10.1080/10236669908009742
39. Gallyamov MO (2011) Scanning force microscopy as applied to conformational studies in macromolecular research. Macromol Rapid Commun 32:1210–1246. doi:10.1002/marc.201100150
40. Gallyamov MO, Yaminskii IV (2001) Quantitative methods for restoration of true topographical properties of objects using the measured AFM-images. 2. The effect of broadening of the AFM-profile. Surf Investig 16:1135–1141. http://arxiv.org/abs/1107.4204v1
41. Rinaudo M (2006) Chitin and chitosan: properties and applications. Prog Polym Sci 31:603–632. doi:10.1016/j.progpolymsci.2006.06.001
42. Abu-Lail NI, Camesano TA (2003) Polysaccharide properties probed with atomic force microscopy. J Microsc 212:217–238. doi:10.1111/j.1365-2818.2003.01261.x
43. Schatz C, Viton C, Delair T, Pichot C, Domard A (2003) Typical physicochemical behaviors of chitosan in aqueous solution. Biomacromolecules 4:641–648. doi:10.1021/bm025724c
44. Crovetto R (1991) Evaluation of solubility data of the system CO_2–H_2O from 273 K to the critical point of water. J Phys Chem Ref Data 20:575–589. doi:10.1063/1.555905
45. Dobrynin AV (2008) Theory and simulations of charged polymers: from solution properties to polymeric nanomaterials. Curr Opin Colloid Interface Sci 13:376–388. doi:10.1016/j.cocis.2008.03.006
46. Borisov OV, Darinskii AA, Zhulina EB (1996) Stretching of polyelectrolyte coils and globules in an elongational flow. Macromolecules 28:7180–7187. doi:10.1021/ma00125a021
47. Pattanayek SK, Pereira GG (2007) Shapes of strongly absorbed polyelectrolytes in poor solvents. Phys Rev E 75:051802. doi:10.1103/PhysRevE.75.051802
48. Minko S, Kiriy A, Gorodyska G, Stamm M (2002) Single flexible hydrophobic polyelectrolyte molecules adsorbed on solid substrate: transition between a stretched chain, necklace-like conformation and a globule. J Am Chem Soc 124:3218–3219. doi:10.1021/ja017767r
49. Kiriy A, Gorodyska G, Minko S, Jaeger W, Štěpánek P, Stamm M (2002) Cascade of coil-globule conformational transitions of single flexible polyelectrolyte molecules in poor solvent. J Am Chem Soc 124:13454–13462. doi:10.1021/ja0261168
50. Roiter Y, Trotsenko O, Tokarev V, Minko S (2010) Single molecule experiments visualizing adsorbed polyelectrolyte molecules in the full range of mono- and divalent counterion concentrations. J Am Chem Soc 132:13660–13662. doi:10.1021/ja106065g
51. Trotsenko O, Roiter Y, Minko S (2012) Conformational transitions of flexible hydrophobic polyelectrolytes in solutions of monovalent and multivalent salts and their mixtures. Langmuir. 28:6037–6044. doi:10.1021/la300584k
52. Akhadov YY (1981) Dielectric properties of binary solutions. Pergamon, Oxford

53. Hasted JB, Roderick GW (1958) Dielectric properties of aqueous and alcoholic electrolytic solutions. J Chem Phys 29:17–26. doi:10.1063/1.1744418
54. Lileev AS, Loginova DV, Lyashchenko AK (2007) Dielectric properties of aqueous hydrochloric acid solutions. Mendeleev Commun 17:364–365. doi:10.1016/j.mencom.2007.11.024
55. Fuoss RM, Kirkwood JG (1941) Electrical properties of solids. VIII. Dipole moments in polyvinyl chloride–diphenyl systems. J Am Chem Soc 63:385–394. doi:10.1021/ja01847a013
56. Michels A, Michels C (1933) The influence of pressure on the dielectric constant of carbon dioxide up to 1000 atmospheres between 25° and 150 °C. Phil Trans R Soc Lond A 231:409–434. doi:10.1098/rsta.1933.0011
57. Saito S (1995) Research activities on supercritical fluid science and technology in Japan—a review. J Supercrit Fluids 8:177–204. doi:10.1016/0896-8446(95)90032-2
58. Kaatze U (1997) The dielectric properties of water in its different states of interaction. J Solution Chem 26:1049–1112. doi:10.1007/BF02768829
59. Wang P, Anderko A (2001) Computation of dielectric constants of solvent mixtures and electrolyte solutions. Fluid Phase Equilibr 186:103–122. doi:10.1016/S0378-3812(01)00507-6
60. Limbach HJ, Holm C (2003) Single-chain properties of polyelectrolytes in poor solvent. J Phys Chem B 107:8041–8055. doi:10.1021/jp027606p
61. Khokhlov AR (1980) On the collapse of weakly charged polyelectrolytes. J Phys A Math Gen 13:979–987. doi:10.1088/0305-4470/13/3/030
62. Manning GS (1969) Limiting laws and counterion condensation in polyelectrolyte solutions I. Colligative properties. J Chem Phys 51:924. doi:10.1063/1.1672157
63. Vasilevskaya VV, Markov VA, Khalatur PG, Khokhlov AR (2006) Semiflexible amphiphilic polymers: cylindrical-shaped, collagen-like, and toroidal structures. J Chem Phys 124:144914. doi:10.1063/1.2191049
64. Markov VA, Vasilevskaya VV, Khalatur PG, ten Brinke G, Khokhlov AR (2008) Conformational properties of rigid-chain amphiphilic macromolecules: the phase diagram. Polym Sci A 50:621–629. doi:10.1134/S0965545X08060059
65. Vasilevskaya VV, Markov VA, ten Brinke G, Khokhlov AR (2008) Self-organization in solutions of stiff-chain amphiphilic macromolecules. Macromolecules 41:7722–7728. doi:10.1021/ma800465j
66. Weinhold MX, Thöming J (2011) On conformational analysis of chitosan. Carbohydr Polym 84:1237–1243. doi:10.1016/j.carbpol.2011.01.011
67. Mauritz KA, Moore RB (2004) State of understanding of Nafion. Chem Rev 104:4535–4585. doi:10.1021/cr0207123
68. Aranson IS, Volfson D, Tsimring LS (2007) Swirling motion in a system of vibrated elongated particles. Phys Rev E 75:051301. doi:10.1103/PhysRevE.75.051301
69. Dolganov PV, Nguyen HT, Kats EI, Dolganov VK, Cluzeau P (2007) Rearrangement of topological defects and anchoring on the inclusion boundary in ferroelectric smectic membranes. Phys Rev E 75:031706. doi:10.1103/PhysRevE.75.031706
70. Semenov AN, Khokhlov AR (1988) Statistical physics of liquid-crystalline polymers. Usp Fiz Nauk 156:427–476. doi:10.3367/UFNr.0156.198811b.0427
71. Raman CV, Krishnan KS (1928) A theory of the birefringence induced by flow in liquids. Philos Mag 5:769–783
72. Chandrasekhar S (1977) Liquid crystals. Cambridge University Press, Cambridge